Dyes and Pigments 80 (2009) 321–328

Contents lists available at ScienceDirect

Dyes and Pigments

journal homepage: www.elsevier.com/locate/dyepig

Novel *meso*-substituted porphyrins: Synthesis, characterization and photocatalytic activity of their TiO_2-based composites

Chen Wang [a], Gao-mai Yang [a], Jun Li [a,*], Giuseppe Mele [b,**], Rudolf Słota [c], Małgorzata A. Broda [c], Ming-yue Duan [a], Giuseppe Vasapollo [b], Xiongfu Zhang [d], Feng-Xing Zhang [a]

[a] *Shaanxi Key Laboratory of Physico-Inorganic Chemistry, Department of Chemistry, Northwest University, Xi'an, Shaanxi 710069, China*
[b] *Dipartimento di Ingegneria dell'Innovazione, Università del Salento, Via Arnesano, 73100 Lecce, Italy*
[c] *Faculty of Chemistry, Opole University, ul. Oleska 48, 45-095 Opole, Poland*
[d] *State Key Laboratory of Fine Chemicals, Dalian University of Technology, Dalian 116012, China*

ARTICLE INFO

Article history:
Received 4 June 2008
Received in revised form 1 August 2008
Accepted 6 August 2008
Available online 26 August 2008

Keywords:
Porphyrins
Metalloporphyrins
Photosensitizer
Photodegradation
DFT calculations
TiO_2

ABSTRACT

Two series of novel *meso*-substituted porphyrins, namely 5,10,15,20-tetra[4-(3-phenoxy)-propoxy]phenyl porphyrin, the structural analogue 5,10,15,20-tetra[2-(3-phenoxy)-propoxy]phenyl porphyrin and their Co(II) Cu(II) and Zn(II) complexes were synthesized. The compounds were characterized using various spectroscopic techniques and their molecular structure was proposed based on density functional theory calculations. The diverse properties of the porphyrin derivatives result from the different stereochemistry of the particular substituents at the *meso* site on the macrocycle and are controlled also by the coordinated metal. The ^{1}H NMR spectrum of the free-base porphyrin showed a complicated spin-splitting. The photocatalytic activities in degradation of 4-nitrophenol were investigated using polycrystalline TiO_2 impregnated with the porphyrins and metalloporphyrins. The Cu(II) porphyrin was a more effective sensitizer than other metal containing compounds (M = Co, Zn) as well as the free-base. Photocatalytic activity was also influenced by spatial positions of the substitutions on the porphyrin molecules.

1. Introduction

For the last half century, porphyrins (Pps) have been widely investigated for their activity toward natural proteins and in enzyme catalysis [1–3]. Owing to the very important role in biological systems, these compounds have been considered very attractive materials for diverse technical and commercial reasons. Synthetic porphyrins in principle preserve the aromatic character of the heterocyclic core formed by the conjugated π-bonding system. However, the overall molecular set-up may be rearranged by either introducing axial ligands and/or other substituents attached to the carbon bridges (*meso* position) or replacing the hydrogens of the pyrrole units. Such modified porphyrin systems have shown a range of interesting physicochemical features, including photoactivity, optoelectronic and electrochemical properties, and hence they are supposed to find application in hi-tech materials [4–11], medical treatment [12–17], molecular recognition [18,19], photosensitizers and photocatalysts [20–26] as well as in different areas of modern technology.

From among the recently developed composite catalysts, polycrystalline TiO_2 impregnated with porphyrin sensitizers proved a very promising alternative to other similar materials explored so far. The porphyrin component enhances the visible light-sensibility of the TiO_2 matrix thus increasing its photocatalytic activity [21,27–29]. Diverse functional groups anchored to the macrocycle were reported to influence the efficiency of TiO_2–Pp systems, depending on the position of the substituent and spacer length [30], occurrence of strong polar groups (*e.g.* –OH, $–SO_3$, RCOO–) [31–35] and also highly electronegative atoms, *e.g.* O or Cl, combined with the pyrrole units [36,37]. In this context, the importance of the coordinated metal is emphasized, as well [38,39].

This paper reports the synthesis of two novel porphyrin series including the free-base compounds **1a** and **1b** (Fig. 1) and their complexes of Co(II), Cu(II) and Zn(II) which were used as sensitizers. The main difference between them is the position of the 3-phenoxy-propoxy group within the *meso*-substituted spacer, which is supposed to affect strongly the porphyrin's stereochemistry. In such cases, the contribution of the entropic factor to the system's reactivity usually proves pronounced. Hence, it seemed obvious that both the series would display diverse catalytic activity. Therefore, we felt reasonable to apply the novel products to impregnate polycrystalline

* Corresponding author. Shaanxi Key Laboratory of Physico-Inorganic Chemistry, Department of Chemistry, Northwest University, Xi'an, Shaanxi 710069, China. Tel.: +86 29 85238119; fax: +86 29 88303798.
** Corresponding author.
E-mail address: junli@nwu.edu.cn (J. Li).

0143-7208/$ – see front matter
doi:10.1016/j.dyepig.2008.08.008

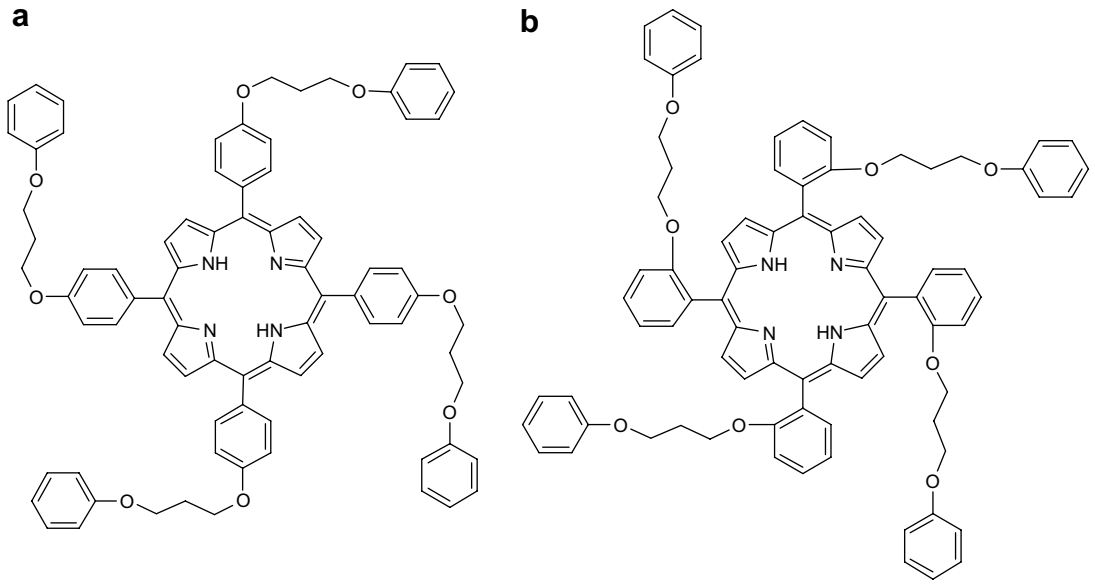

Fig. 1. Chemical structure of the novel free-base porphyrins (H_2Pp) **1a** and **1b**.

TiO_2 (anatase) and thus evaluate their effectiveness in photodegradation of 4-nitrophenol in water, in a process sensitized by visible light. To assess the structural effects, we have optimized the molecular structure of both the porphyrin isomers by means of density functional theoretical (DFT) calculations.

2. Experimental

2.1. Materials and methods

2,3-Dichloro-5,6-dicyano-1,4-benzoquinone (DDQ) (Aldrich) and other reagents (Beijing Chemical Reagents Company) were used without further purification, except pyrrole, which was distilled before use. Impregnated TiO_2 – anatase (Ti oxide Huntsman), BET specific surface area 8 m^2/g, was used in preparation of loaded samples applied as photocatalysts in photoreactivity experiments.

Cu(II) 5,10,15,20-tetrakis(4-*tert*-butylphenyl) porphyrin, for brevity denoted CuPp(c), was synthesized according to the procedure reported in the literature [25], and the Cu(II) tetraphenylporphyrin, for brevity denoted CuPp(d), was synthesized according to the usual methods.

Elemental analysis (C, H, N) was performed by a Vario EL-III CHNOS instrument. FT-IR spectra were registered in KBr using a BEQ UZNDX-550. UV–vis spectra were recorded by a Shimadzu UV2550 spectrophotometer. ^{1}H NMR spectra were recorded at room temperature using a Bruker AC-400 apparatus and tetramethyl silane (TMS) for reference.

Mass spectrometry (MS) analyses were carried out on a matrix assisted laser desorption/ionization time of flight mass spectrometer (MALDI-TOF MS, Krato Analytical Company of Shimadzu Biotech) using a standard procedure involving 1 μL of the sample solution. Specific surface area was measured by the single point BET method using a jw-05 apparatus (Beijing, China). Total organic carbon (TOC) was measured using TOC Analytical (OI Analytical Company, USA).

2.2. Synthesis of porphyrins ***1a***, ***1b*** and metalloporphyrins

2.2.1. Preparation of ***2***

3-Phenoxypropyl bromide (**2**) was synthesized according to Ref. [40] (Scheme 1). Phenol (28.0 g, 0.3 mol) and 37.7 mL (0.37 mol) of 1,3-dibromopropane in 150 mL of H_2O were heated under stirring at 100 °C in an oil bath; at the same time a solution of 11.3 g (0.28 mol) NaOH in 40 mL of water was dropwise added into the reaction system within 30 min. The mixture was refluxed for 4 h, then the water layer was separated off and the remaining oil layer was distilled under vacuum. After the unreacted 1,3-dibromopropane was distilled off, the 3-phenoxypropyl bromide (**2**) was successively collected as a colorless oil liquid. Yield: 85%; Mp: 10–11 °C; n_{20}^D: 1.5460. Anal. Calcd. for $C_9H_{11}BrO$, %: C, 50.30; H, 5.09. Found C, 50.26; H, 5.15.

2.2.2. Preparation of ***3a*** and ***3b***

4-Hydroxybenzaldehyde (10.0 g, 0.082 mol) and 3-phenoxypropyl bromide (**2**) (12.5 mL, 0.08 mol) in 100 mL of CH_3CH_2OH were heated under stirring at 80 °C in a water bath, then 3.2 g (0.08 mol) of NaOH dissolved in 50 mL CH_3CH_2OH was dropped into the reaction system within 1 h and the mixture was refluxed for 6 h. After cooling, the mixture was washed with distilled water for several times and next the solvent was removed under vacuum. The remaining oily liquid was dissolved in ethanol. Colorless crystals of 4-(3-phenoxy) propoxybenzaldehyde (**3a**) were obtained from the solution. The same procedure was used for the synthesis of 2-(3-phenoxy)propoxybenzaldehyde (**3b**) from **2** and 2-hydroxybenzaldehyde.

Yield (**3a**): 38%. Mp: 60–61 °C; Anal. Calcd. for $C_{19}H_{16}O_3$, %: C, 75.32; H, 6.32. Found C, 74.98; H, 6.29. FT-IR: ν, cm^{-1} 2952, 2836, 2749, 1698, 1602, 1502, 1464, 1384, 1160, 1060, 830, 754. ^{1}H NMR ($CDCl_3$, 300 MHz): δ, ppm 7.82 (d, $J = 8.43$ Hz, 2H, Ar), 7.28 (t, $J = 7.88$ Hz, 2H, Ar), 7.05–6.85 (m, 5H, Ar), 4.26 (t, $J = 6.02$ Hz, 2H, OCH_2), 4.17 (t, $J = 5.84$ Hz, 2H, OCH_2), 2.30 (quintuplet, $J = 5.62$ Hz, 2H, CH_2).

Yield (**3b**): 35%. Mp: 53–54 °C. Anal. Calcd. for $C_{19}H_{16}O_3$, %: C, 75.30; H, 6.35. Found C, 74.98; H, 6.29. FT-IR: ν, cm^{-1} 2932, 2873, 2768, 1685, 1600, 1487, 1458, 1386, 1187, 1058, 808, 760. ^{1}H NMR ($CDCl_3$, 300 MHz): δ, ppm 7.84 (t, $J = 6.27$ Hz, 1H, Ar), 7.53 (t, $J = 6.81$ Hz, 1H, Ar), 7.28 (t, $J = 7.50$ Hz, 2H, Ar), 7.10–6.85 (m, 5H, Ar), 4.30 (t, $J = 6.02$ Hz, 2H, OCH_2), 4.19 (t, $J = 5.91$ Hz, 2H, OCH_2), 2.38–2.32 (m, 2H, CH_2).

2.2.3. Synthesis of the free-base porphyrins ***1a*** and ***1b*** (H_2Pps)

4-(3-Phenoxy)propoxybenzaldehyde (**3a**) (2.13 g, 8.3 mmol) and pyrrole (0.56 mL, 8.3 mmol) in 200 mL of chloroform were first stirred at room temperature for 10 min under nitrogen atmosphere.

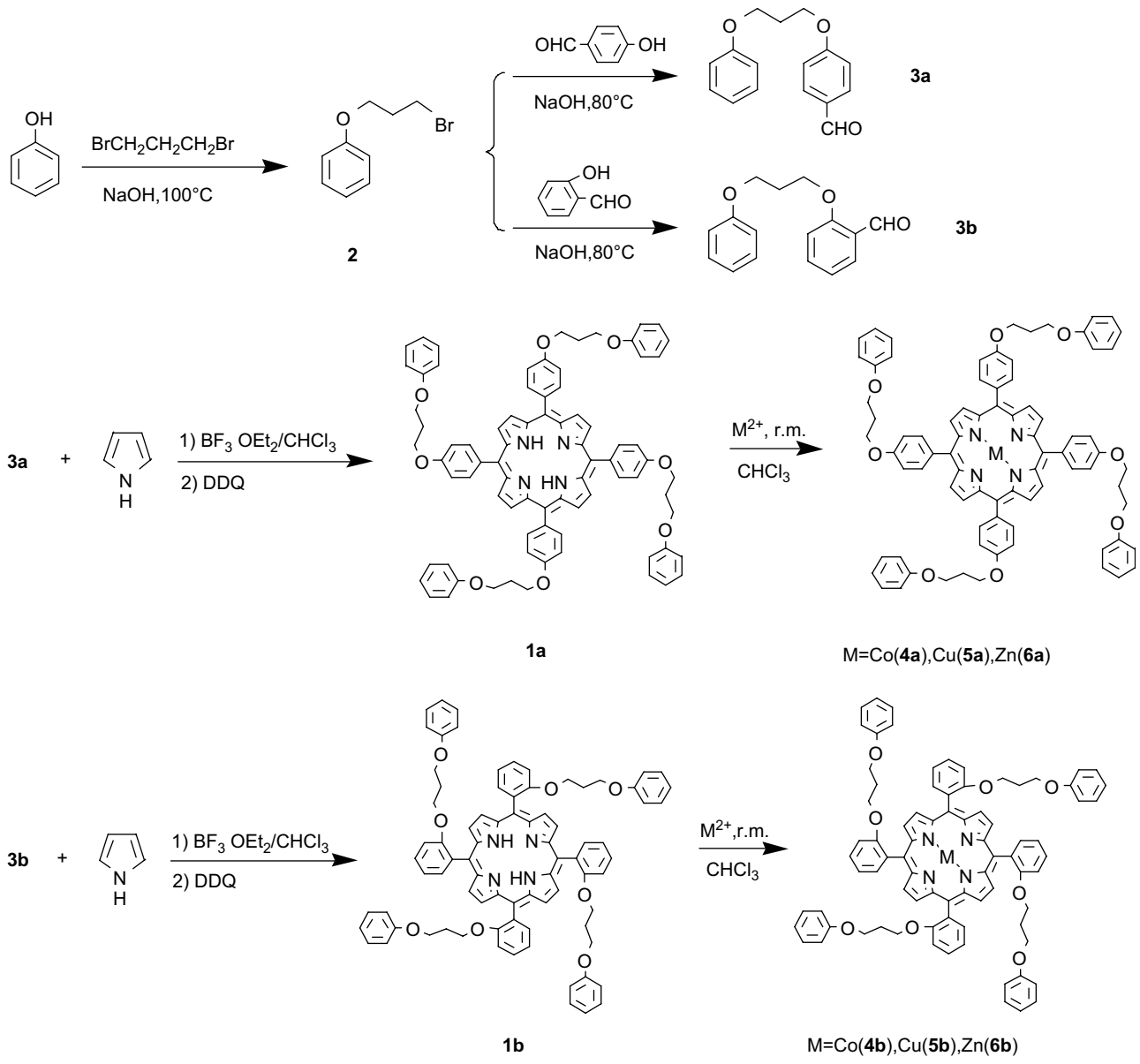

Scheme 1. Synthesis of porphyrins **1a**, **1b** and metalloporphyrins.

Then 0.13 mL (2.8 mmol) of $BF_3 \cdot OEt_2$ in 5 mL of $CHCl_3$ was added. The reaction mixture was stirred at room temperature for 40 h and successively for another 50 h after addition of 1.4 g (6.16 mmol) of DDQ. The solvent was removed under vacuum and the crude product, **1a**, was purified by chromatography on a silica gel column with CH_2Cl_2/ethanol (35/1 vv) as eluant. The synthesis of **1b** was carried out in a similar way starting with **3b**.

*2.2.3.1. 5,10,15,20-Tetra[4-(3-phenoxy)-propoxy]phenyl porphyrin (**1a**).* Yield: 15%. Mp: >250 °C, Anal. Calcd. for $C_{80}H_{70}N_4O_8$, %: C, 79.11; H, 5.68; N, 4.58. Found C, 79.10; H, 5.80; N, 4.61. FT-IR: ν, cm^{-1} 3315.77, 3060.12, 2924.96, 2361.51, 1595.37, 1493.20, 1287.02, 1241.83, 1052.85, 964.01, 751.63. ^1H NMR ($CDCl_3$, 400 MHz): δ, ppm 8.83 (s, 8H, β position of the pyrrole moiety), 8.09 (d, $J = 8.6$ Hz, 8H, Ar), 7.40–7.22 (m, 16H, Ar), 7.03–6.95 (m, 12H, Ar), 4.45 (t, $J = 6.0$ Hz, 8H, OCH_2), 4.33 (t, $J = 6.0$ Hz, 8H, OCH_2), 2.43 (quintuplet, $J = 6.0$ Hz, 8H, CH_2), −2.78 (br s, 2H, NH). MS and UV–vis ($CHCl_3$) data: see Table 1.

*2.2.3.2. 5,10,15,20-Tetra[2-(3-phenoxy)-propoxy]phenyl porphyrin (**1b**).* Yield: 10%. Mp: >250 °C, Anal. Calcd. for $C_{80}H_{70}N_4O_8$, %: C, 79.14; H, 5.733; N, 4.62. Found C, 79.10; H, 5.805; N, 4.61. ^1H NMR ($CDCl_3$, 400 MHz): δ, ppm 8.70–8.64 (m, 8H, β position of the pyrrole moiety), 7.97–7.84 (m, 4H, Ar), 7.78–7.72 (m, 4H, Ar), 7.39–7.27 (m, 8H, Ar), 6.76–6.60 (m, 6H, Ar), 6.59–6.47 (m, 6H, Ar), 6.19–5.90 (m, 8H, Ar), 4.14–3.96 (m, 8H, OCH_2), 2.98–2.78 (m, 8H, OCH_2), 1.48–1.20 (m, 8H, CH_2), −2.63 (br s, 2H, NH). MS and UV–vis ($CHCl_3$) data: see Table 1.

Table 1
Mass and UV–vis spectral data of the synthesized porphyrins

Compounds	M	*m/z* (amu)	λ_{max} (nm)				
1a	H	1214.4	423	519	556	593	649
1b	H	1214.2	419	514	548	589	644
4a	Co	1273.3	412		529		
4b	Co	1273.6	410		530		
5a	Cu	1277.9	419		541	579	
5b	Cu	1277.6	417		540	575	
6a	Zn	1279.8	422		549	584	
6b	Zn	1279.2	423		550	588	
CuPp(c)	Cu		417		540	576	
CuPp(d)	Cu		411		538	574	

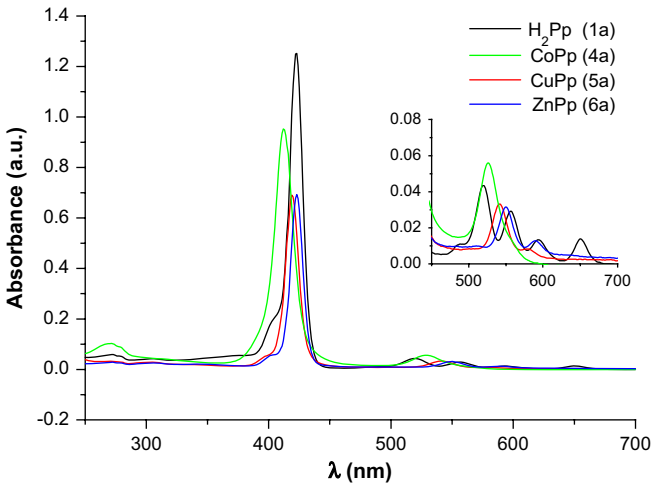

Fig. 2. The UV–vis spectra of H_2Pp (**1a**) and MPps (**4a**–**6a**).

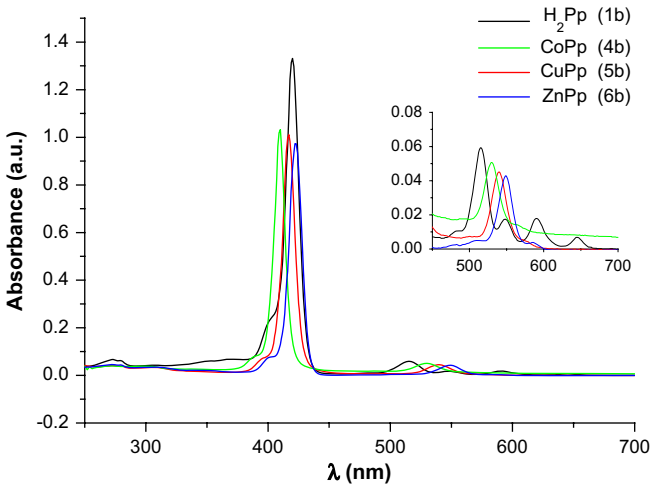

Fig. 3. The UV–vis spectra of H_2Pp (**1b**) and MPps (**4b**–**6b**).

*2.2.4. Synthesis of the metalloporphyrins **4a**, **5a**, **6a** and **4b**, **5b** and **6b***

$CuCl_2$ (27.0 mg, 0.15 mmol) was added to **1a** or **1b** (60.8 mg, 0.05 mmol) dissolved in 20 mL of $CHCl_3$ and 3 mL of ethanol. The mixture was stirred for 24 h at room temperature and monitored by TLC until the complete disappearance of the starting material (**1a** or **1b**). The unreacted solid salt was filtered off and the solvent was removed under vacuum. The crude product, **5a** or **5b**, respectively, was purified by chromatography on a silica gel column with CH_2Cl_2 as eluant. Both the CoPp compounds, **4a** and **4b**, were obtained using $Co(OAc)_2$ and **1a** or **1b**, respectively, according to the same method as described above. Both the ZnPp complexes, **6a** and **6b**, were prepared from $Zn(OAc)_2$ and **1a** or **1b**, respectively, following the same procedure.

*2.2.4.1. Co(II) 5,10,15,20-tetra[4-(3-phenoxy)-propoxy]phenyl porphyrin (**4a**).* Yield: 88%. Mp >250 °C, Anal. Calcd. for $CoC_{80}H_{68}N_4O_8$, %: C, 75.42; H, 5.10; N, 4.57. Found C, 75.55; H, 5.40; N, 4.41. MS and UV–vis ($CHCl_3$) data: see Table 1.

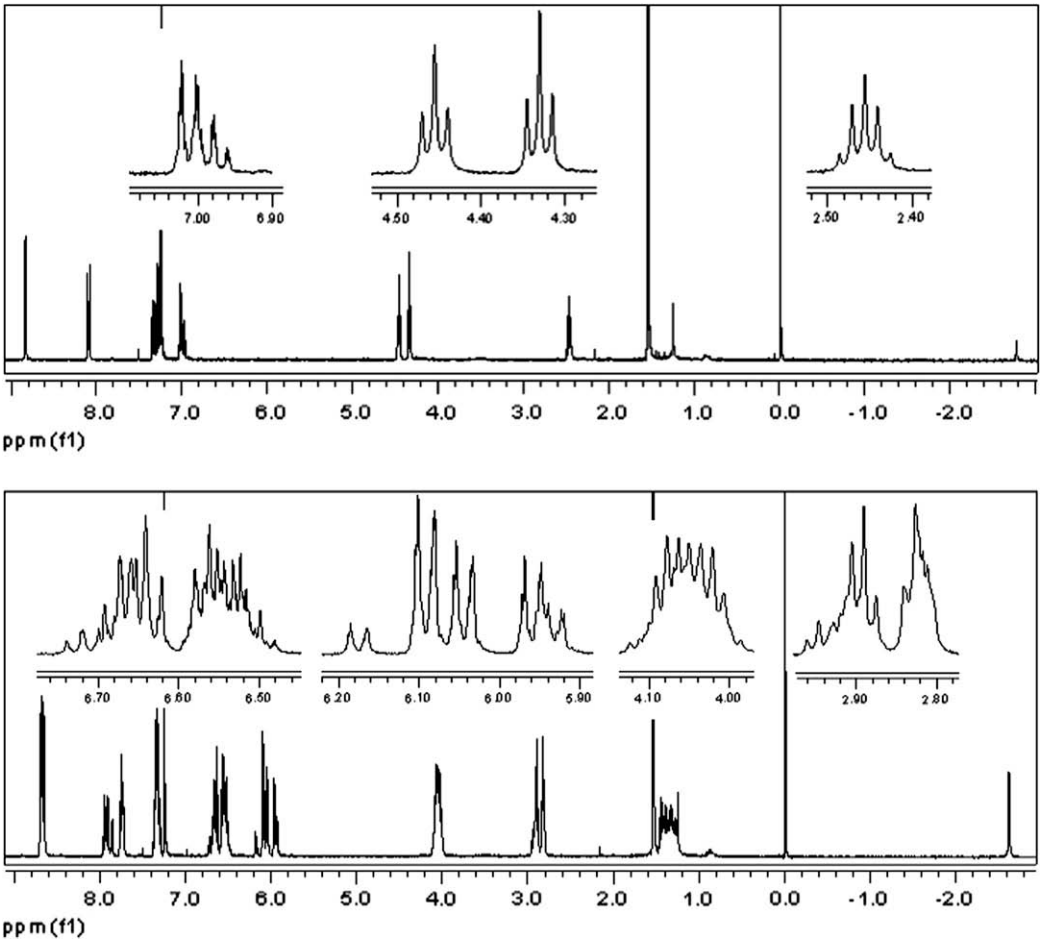

Fig. 4. ^1H NMR spectra of **1a** (top) and **1b** (bottom).

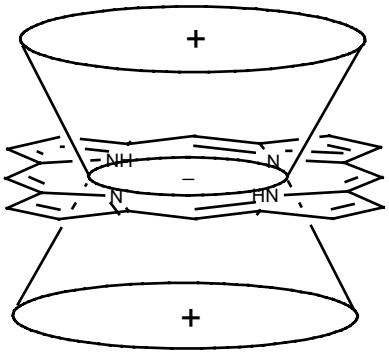

Fig. 5. The anisotropic effect of the porphyrin ring.

*2.2.4.2. Co(II) 5,10,15,20-tetra[2-(3-phenoxy)-propoxy]phenyl porphyrin (**4b**).* Yield: 90%. Mp >250 °C, Anal. Calcd. for $CoC_{80}H_{68}N_4O_8$, %: C, 75.36; H, 5.28; N, 4.52. Found C, 75.55; H, 5.40; N, 4.41. MS and UV–vis ($CHCl_3$) data: see Table 1.

*2.2.4.3. Cu(II) 5,10,15,20-tetra[4-(3-phenoxy)-propoxy]phenyl porphyrin (**5a**).* Yield: 92%. Mp: >250 °C, Anal. Calcd. for $CuC_{80}H_{68}N_4O_8$, %: C, 75.08; H, 5.54; N, 4.19. Found C, 75.24; H, 5.38; N, 4.39. MS and UV–vis ($CHCl_3$) data: see Table 1.

*2.2.4.4. Cu(II) 5,10,15,20-tetra[2-(3-phenoxy)-propoxy]phenyl porphyrin (**5b**).* Yield: 90%. Mp >250 °C, Anal. Calcd. for $CuC_{80}H_{68}N_4O_8$, %: C, 75.13; H, 5.64; N, 4.47. Found C, 75.24; H, 5.37; N, 4.39. MS and UV–vis ($CHCl_3$) data: see Table 1.

*2.2.4.5. Zn(II) 5,10,15,20-tetra[4-(3-phenoxy)-propoxy]phenyl porphyrin (**6a**).* Yield: 90%. Mp >250 °C, Anal. Calcd. for $ZnC_{80}H_{68}N_4O_8$, %: C, 75.40; H, 5.66; N, 4.43. Found C, 75.17; H, 5.37; N, 4.38. MS and UV–vis ($CHCl_3$) data: see Table 1.

*2.2.4.6. Zn(II) 5,10,15,20-tetra[2-(3-phenoxy)-propoxy]phenyl porphyrin (**6b**).* Yield: 90%. Mp >250 °C, Anal. Calcd. for $ZnC_{80}H_{68}N_4O_8$, %: C, 75.35; H, 5.67; N, 4.42. Found C, 75.17; H, 5.37; N, 4.38. MS and UV–vis ($CHCl_3$) data: see Table 1.

2.3. Preparation of the photocatalysts

All porphyrins and metalloporphyrins were used to prepare the TiO_2 composites. Compound **1b** (or **4b**–**6b**, **5a**) (6 μmol) was dissolved in 30 mL of $CHCl_3$ and 1 g finely ground TiO_2 was added to this solution. The resulting suspension was stirred for 4–5 h and then the photocatalyst was separated from the solution by centrifugation. These photocatalysts were marked as H_2Pp(**1b**)–TiO_2, CoPp(**4b**)–TiO_2, CuPp(**5b**)–TiO_2, ZnPp(**6b**)–TiO_2, CuPp(**5a**)–TiO_2, respectively. The previously synthesized Cu(II) 4-*tert*-butylphenyl porphyrin CuPp(c) and Cu(II) tetraphenyl porphyrin CuPp(d) were also used to impregnate TiO_2, marked as CuPp(c)–TiO_2, CuPp(d)–TiO_2, and they served for comparative reasons.

2.4. Photodegradation experiments

The experimental set-up and the applied procedures have been described in detail in the literature [41].

2.5. Theoretical calculations and structure optimization

Density functional theory (DFT) method was applied to calculate the molecular structures of **1a**, **1b** and of their Cu-complexes (**5a** and **5b**). The Becke three-parameter exchange functional (B3) [42] and the Lee–Yang–Parr correlation functional (LYP) [43] were used along with the GAUSSIAN 03 package [44]. Geometry optimization and vibrational analysis of the studied compounds were performed without constraints on isolated molecules with the LANL2DZ basis set [45]. All normal frequencies at the optimized geometry are real, showing that it is indeed a stable minimum.

3. Results and discussion

3.1. Synthesis and compounds' characterization

The synthetic route has been illustrated in Scheme 1. The precursors (**2**, **3a** and **3b**) were easily prepared and purified. However, the Lindsay method [46], applied to obtain the free-base porphyrins (**1a** and **1b**) provided rather low yields (15 and 10%, respectively). Nevertheless, the metalloporphyrins were all synthesized with yields around 90%.

The data collected in Table 1 are well consistent with the molecular structure of the synthesized porphyrins. Mass spectroscopy data perfectly correspond to the expected *m*/*z* values for the individual products. UV–vis spectra show features typical for this class of compounds and the influence of the *meso* substituent upon the position of absorption bands has proved insignificant

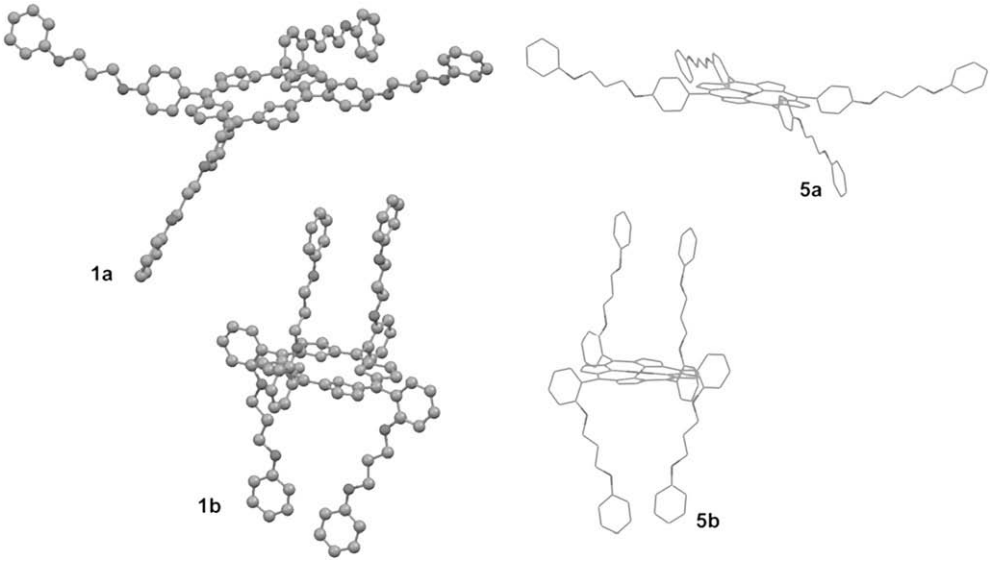

Fig. 6. Molecular structure of the novel [(3-phenoxy)-propoxy]phenyl porphyrins: H_2Pp (**1a**, **1b**) and CuPp (**5a**, **5b**).

(Figs. 2 and 3). In fact, one may note some slight spectral shifts by comparing the corresponding "**a**" and "**b**" isomers, especially for both the H_2Pp species (**1a** and **1b**). The H_2Pp (**1a**) shows a band centered at $\lambda = 423$ (Soret band), and the Q bands absorptions, respectively, at 519, 556, 593 and 649 nm which has the weak einstein shift compared with the H_2Pp (**1b**) UV–vis spectrum of consists of a Soret band at 419 nm, and Q bands at 514, 548, 589, 644 nm. Since the metal derivatives produce a more rigid electronic structure of the porphyrin core, therefore spacer-related spectral effects are much less pronounced, The Q band peaks number decrease from four to two (CuPp, ZnPp) or one (CoPp), and a violet shift were also observed in metalloporphyrins, as shown in Table 1.

FT-IR and ^1H NMR spectra were also consistent with the structure of the synthesized compounds. Particularly the ^1H NMR spectra have appeared very interesting (Fig. 4). Due to the porphyrin ring anisotropic effect, resulting from circulation of electrons making up the conjugated π-bonding system, two shielded zones are formed, over and under the macrocycle plane (Fig. 5). The chemical shift assigned to protons falling within the conical areas are shielded, and those falling outside the conical areas are deshielded. In this way it was possible to justify the chemical shifts measured in the case of **1b** which are shielded for 0.1–1.2 ppm relatively to **1a**. Indeed, the optimized molecular structures presented in Fig. 6 and Table 2 indicate that in **1b** the 3-phenoxypropoxy spacers evidently lie within the range of the shielded zone, whereas in **1a** they do not. For the same reason the spectrum of **1b** has shown a more complex spin-splitting pattern than that of **1a**. Note especially the characteristic splitting of the H–Ar peaks, which in **1b** consists of six multiplets within the range from 7.97 to 5.9 ppm, whereas in **1a** only three such groups have been featured, 8.09 (d, $J = 8.6$ Hz, 8H), 7.40–7.22 (m, 16H) and 7.03–6.95 (q, 12H).

3.2. Molecular structure

Theoretical calculations allowed estimating the structural parameters of both the synthesized isomers of the free-base porphyrin (H_2Pp) and their copper complexes (CuPp). Some results have been collected in Table 2 and the appropriate structures are depicted in Fig. 6.

It is obvious the structure of **1b** is more stressed than in the case of **1a**, which follows from evidently stronger steric interactions between the *cis meso*-substituents in **1b**, separated from each other at the peripheral phenyls by a distance less than the size of the porphyrin core. The same conclusions apply also to both the copper complexes, **5a** and **5b**. In all presented cases, the macrocycles were found somewhat wrinkled and the deviation from perfect planarity seems to be the strongest for **5b**. There are apparent differences in torsion angles between the plane determined by the four pyrrole N atoms and the plane of the *meso*-substituted phenyls. Interestingly,

Table 2
Structural parameters and size of the H_2Pp and CuPp molecules

Distance (Å)	H_2Pp		CuPp	
	1a	**1b**	**5a**	**5b**
N–N[a]	4.162	4.152	4.060	4.050
C–C[b]	6.996	6.972	6.970	6.940
Phen–phen[c]	*cis* 34.044	*cis* 4.182 *trans* 23.118	*cis* 34.868	*cis* 4.110 *trans* 23.021
Torsion angle (°)				
μ-phen–Pc[d]	62.7–117.1	83.1–95.0	64.6–120.0	81.7–100.0
C–O–μ-phen[e]	0	0.3–2.9	0	0.2–2.7

[a] Opposite atoms (mean value).
[b] Opposite *meso*-C atoms (mean value).
[c] Longest and/or shortest distance between the peripheral phenyls.
[d] The *meso*-phenyl plane vs. Pc plane.
[e] Measured about the O–phen bond.

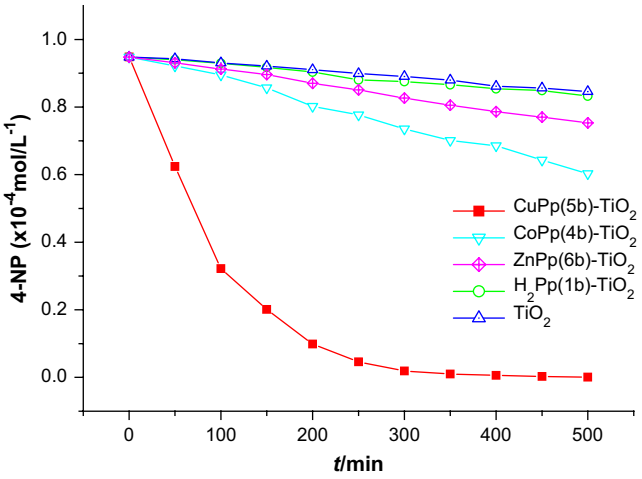

Fig. 7. 4-NP concentration vs. irradiation time using different MPp photocatalysts.

the *meso*-phenyls are considerably inclined in the case of **1a** and **5a**, whereas for **1b** and **5b** they are almost perpendicular to the porphyrin plane. Moreover, in **1b** and **5b** the spacers are also twisted to some extent about the O–C (phen) bond axis (0.2–2.9°) so that both the terminal-phenyls are not coplanar, as they do appear in **1a** and **5a**.

3.3. Photoreactivity experiments

The photocatalytic activities for the degradation of 4-nitrophenol (4-NP) in water under visible light irradiation using prepared photocatalysts were tested. As expected, the Cu(II) porphyrin (**5b**) definitely proved more effective sensitizers in photodegradation of 4-nitrophenol than other MPp's (M = Co, Zn) as well as the free-base H_2Pp (Fig. 7). The Co(II), Zn(II) porphyrins (**4b**, **6b**) have slight beneficial effect, and there is no remarkable effect on the free-base porphyrin (**1b**) compared with bare TiO_2, these results are similar to our previous studies [47].

The photocatalytic activities are also influenced by the substitutions and the spatial positions of the substitutions of porphyrins. As shown in Fig. 8, all the Cu(II) porphyrins including the novel Cu–porhyrins (**5a**, **5b**) revealed better photocatalytic activity under visible light irradiation for the degradation of 4-nitrophenol (4-NP) in water. The efficiency of the catalyst was found to decrease in the following order.

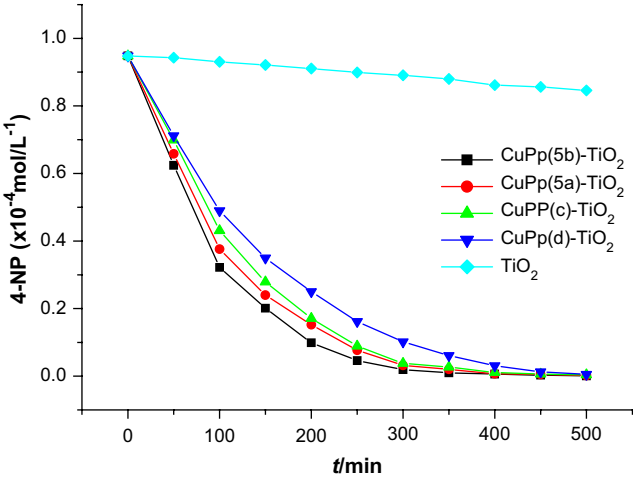

Fig. 8. 4-NP concentration vs. irradiation time using different CuPp photocatalysts.

Table 3
The initial photoreaction rates and the conversion (%) of 4-NP after 250 and 500 min of irradiation time

Samples	$r_0 \times 10^9$ (mol L^{-1} s^{-1})	$r_0' \times 10^9$ (mol L^{-1} s^{-1} m^{-2})	4-NP (%) converted, 250 min	4-NP (%) converted, 500 min	TOC (%), 250 min	TOC (%), 500 min
TiO_2	0.16	1	5.1	10.7	0	0
H_2Pp(**1a**)–TiO_2	0.16	1	4.5	9.9	0	0
H_2Pp(**1b**)–TiO_2	0.25	1.56	7.1	12.1	0	1
ZnPp(**6a**)–TiO_2	0.40	2.50	7.6	14.5	0	2
ZnPp(**6b**)–TiO_2	0.55	3.44	10.2	20.5	1	2
CoPp(**4a**)–TiO_2	0.57	3.564	10.2	20.4	1	2
CoPp(**4b**)–TiO_2	0.87	5.44	18.0	36.4	2	3
CuPp(d)–TiO_2	7.87	49.19	82.9	99.4	17	53
CuPp(c)–TiO_2	8.30	51.88	90.6	99.6	24	62
CuPp(**5a**)–TiO_2	9.67	60.44	91.9	99.8	29	70
CuPp(**5b**)–TiO_2	10.80	67.50	95.1	99.9	34	76

r_0: the initial photoreaction rates per used mass.
r_0': the initial photoreaction rates per used mass and per unit surface area of the catalysts.

CuPp(**5b**)–TiO_2 > CuPp(**5a**)–TiO_2 > CuPp(c)–TiO_2 > CuPp(d)–TiO_2 > TiO_2 (bare).

The initial zeroth order reaction rates [22] for 4-NP disappearance per used mass of the catalysts (r_0), per square meter of powder (r_0'), the conversion percentage of 4-NP after 250 and 500 min and the decreasing total organic carbon measurements (TOC) are reported in Table 3. The data displayed the difference of the photocatalytic activity obviously.

The process on CuPp–TiO_2 photocatalyst is generally accepted to proceed according to the scheme:

$$TiO_2[CuPp] \xrightarrow{h\nu} TiO_2[CuPp]^* + 4\text{-NP}(H_2O, O_2) \rightarrow \text{oxidation products}$$

as proved by the analysis of total organic carbon (TOC). After 250 and 500 min from the start of the photosensitized reaction the corresponding TOCs (%) determined in the studied samples were amounted to 34 and 76 (**5b**), 29 and 70 (**5a**), 24 and 62 (CuPp(c)) and 17 and 53 (CuPp(d)). These results indicate distinctly for the most efficient production of reactive oxidants (*e.g.* $O_2^{\bullet-}$, $OH^{\bullet}$, H_2O_2 or $^1O_2$, [25]) by the composite including **5b**. Presumably, in the case of **5b** the transfer of electrons from the excited porphyrin into the TiO_2 matrix is more effective in comparison with the other compounds used.

The influence of the kind of the *meso* substituent and thus the molecular structure of the porphyrin component upon the system's reactivity is obvious. Long and flexible spacers of **5a** and **5b** may prevent these porphyrins from intermolecular π–π interactions and the consequent decreasement of aggregation if compared with CuPp(c). This particularly occurs for the **5b** complex representing a stereochemically more complicated molecular structure having a lower symmetry and a more stressed bonding system. Such features are considered crucial to assure higher activity of the composite catalyst. Hence, one may expect **5b** to manifest enhanced ability to trap molecular oxygen and in consequence to increase the amount of reactive oxidants, necessary for the degradation of 4-NP in water. Moreover, the way the porphyrins are distributed over the TiO_2 surface and fixed to the matrix is also very important as far as the intermolecular electron transfer is concerned. It follows from our study, that also in this case the molecular system of **5b** is favored over the other ones.

4. Conclusion

The novel [(3-phenoxy)-propoxy]phenyl porphyrins represent two completely diverse molecular systems and thus different physicochemical properties. All of them bear evidence for some stress within the bonding set-up of the porphyrin core, most pronounced in the case of molecules containing the *o*-substituted spacers, *i.e.* [2-(3-phenoxy)-propoxy]phenyl substituents. Results of theoretical calculations (DFT) and ^1H NMR spectroscopy indicate for the importance of the stereochemical factor in reactivity development in porphyrin derivatives. As for the photocatalytic activities, firstly, the more important part is that the excited Cu(II)Pp potential match better with TiO_2 conduction band potential than Co(II)Pp and Zn(II)Pp. secondly, the long and flexible substitution can be impregnated onto the surface of the TiO_2 more effectively than short ones. Thirdly, the spatial positions of the substitutions also influence the impregnated effect of the photosensitizer with the TiO_2. All the factors lead to the following result: Photocatalytic activities of the CuPp–TiO_2 composites proved to rely evidently on structural features of the porphyrin as reflected by the Cu(II) 5,10,15,20-tetra[2-(3-phenoxy)-propoxy]phenyl porphyrin (**5b**), which appeared the most efficient sensitizer.

Acknowledgment

This research was supported by the State Key Laboratory of Fine Chemicals, China and the Educational Committee Foundation of Shaanxi Province. Theoretical calculations were supported by the grant obtained from the Academic Computer Center CYFRONET AGH Kraków, no. KBN/SGI2800/UOpolski/012/2001.

References

[1] Breslow R, Yang J, Yan JM. Biomimetic hydroxylation of saturated carbons with artificial cytochrome P-450 enzymes – liberating chemistry from the tyranny of functional groups. Tetrahedron 2002;58:653–9.
[2] Ambroise A, Li JZ, Yu LH, Lindsey JS. A self-assembled light-harvesting array of seven porphyrins in a wheel and spoke architecture. Organic Letters 2000;2:2563–6.
[3] Qiu WG, Li ZF, Bai GM, Meng SN, Dai HX, He H. Study on the inclusion behavior between *meso*-tetrakis[4-(3-pyridiniumpropoxy)phenyl]prophyrin tetrakis-bromide and β-cyclodextrin derivatives in aqueous solution. Spectrochimica Acta Part A Molecular and Biomolecular Spectroscopy 2007;66:1189–93.
[4] Ishida T, Morisaki Y, Chujo Y. Synthesis of covalently bonded nanostructure from two porphyrin molecular wires leading to a molecular tube. Tetrahedron Letters 2006;47:5265–8.
[5] Guldi DM. Biomimetic assemblies of carbon nanostructures for photochemical energy conversion. Journal of Physical Chemistry B 2005;109:11432–41.
[6] Hasobe T, Kamat PV, Troiani V, Solladie N, Ahn TK, Kim SK, et al. Enhancement of light-energy conversion efficiency by multi-porphyrin arrays of porphyrin-peptide oligomers with fullerene clusters. Journal of Physical Chemistry B 2005;109:19–23.
[7] Takechi K, Shiga T, Motohiro T, Akiyama T, Yamada S, Nakayama H, et al. Solar cells using iodine-doped polythiophene–porphyrin polymer films. Solar Energy Materials and Solar Cells 2006;90:1322–30.
[8] Ogawa K, Zhang TQ, Yoshihara K, Kobuke Y. Large third-order optical nonlinearity of self-assembled porphyrin oligomers. Journal of the American Chemical Society 2002;124:22–3.
[9] Li Y, Cao LF, Tian H. Fluoride ion-triggered dual fluorescence switch based on naphthalimides winged zinc porphyrin. Journal of Organic Chemistry 2006;71:8279–82.

[10] Li JZ, Tang T, Li F, Li M. The synthesis and characterization of novel liquid crystalline, *meso*-tetra[4-(3,4,5-trialkoxybenzoate)phenyl]porphyrins. Dyes and Pigments 2008;77:395–401.
[11] Sun XD, Chen GD, Zhang JL. The photophysical properties of metal complexes of fluoresceineporphyrin dyads. Dyes and Pigments 2008;76:499–501.
[12] Macdonald IJ, Dougherty TJ. Basic principles of photodynamic therapy. Journal of Porphyrins and Phthalocyanines 2001;5:105–29.
[13] Dudkowiak A, Teslak E, Habdas J. Photophysical studies of tetratolylporphyrin photosensitizers for potential medical applications. Journal of Molecular Structure 2006;792–793:93–8.
[14] Tashiro K, Aida T, Zheng JY, Kinbara K, Saigo K, Sakamoto S, et al. A cyclic dimer of metalloporphyrin forms a highly stable inclusion complex with C_{60}. Journal of the American Chemical Society 1999;121:9477–8.
[15] Petritsch K, Friend RH, Lux A, Rozenderg G, Moratti SC, Holmes AB. Liquid crystalline phthalocyanines in organic solar cells. Synthetic Metals 1999;102:1776.
[16] Zhang J, Wu X, Cao X, Yang F, Wang J, Zhou X, et al. Synthesis and antibacterial study of 10,15,20-triphenyl-5-{4-hydroxy-3-(trimethylammonium) methyl}-phenylporphyrin as models for combination of porphyrin and alkylating agent. Bioorganic and Medicinal Chemistry Letters 2003;13:1097–100.
[17] Arap W, Pasqualini R, Ruoslahti E. Cancer treatment by targeted drug delivery to tumor vasculature in a mouse model. Science 1998;279:377–80.
[18] Chen H, Shao XB, Jiang XK, Le ZT. A general approach to L-tyrosine porphyrins. Tetrahedron 2003;59:3505–10.
[19] Kuroda Y, Kawashima A, Hayashi Y, Ogoshi H. Self-organized porphyrin dimer as a highly specific receptor for pyrazine derivatives. Journal of the American Chemistry Society 1997;119:4929–33.
[20] Deng HH, Lu ZH. Heteroaggregation and photoelectric conversion of porphyrins on a nanostructured TiO_2 electrode. Supramolecular Science 1998;5:669–74.
[21] Kira A, Tanaka M, Umeyama T, Matano Y, Yoshimoto N, Zhang Y, et al. Hydrogen-bonding effects on film structure and photoelectrochemical properties of porphyrin and fullerene composites on nanostructured TiO_2 electrodes. Journal of Physical Chemistry C 2007;111:13618–26.
[22] Mele G, Del SR, Vasapollo G, Marcì G, García-López E, Palmisano L, et al. TRMC, XPS, and EPR characterizations of polycrystalline TiO_2 porphyrin impregnated powders and their catalytic activity for 4-nitrophenol photodegradation in aqueous suspension. Journal of Physical Chemistry B 2005;109:12347–52.
[23] Liu X, Liu JH, Pan JX, Andersson S, Sun LC. Synthesis, electrochemical, and photophysical studies of multicomponent systems based on porphyrin and ruthenium(II) polypyridine complexes. Tetrahedron 2007;63:9195–205.
[24] Mele G, Del SR, Vasapollo G, García-López E, Palmisano L, Mazzetto SE, et al. Polycrystalline TiO_2 impregnated with cardanol-based porphyrins for the photocatalytic degradation of 4-nitrophenol. Green Chemistry 2004;6:604–9.
[25] Mele G, Del SR, Vasapollo G, García-López E, Palmisano L, Schiavello M. Photocatalytic degradation of 4-nitrophenol in aqueous suspension by using polycrystalline TiO_2 impregnated with functionalized Cu(II)–porphyrin or Cu(II)–phthalocyanine. Journal of Catalysis 2003;217:334–42.
[26] Cho Y, Choi W, Lee CH, Hyeon T, Lee HI. Visible light-induced degradation of carbon tetrachloride on dye-sensitized TiO_2. Environment Science and Technology 2001;35:966–70.
[27] Wang Q, Campbell WM, Bonfantani EE, Jolley KW, Officer DL, Walsh PJ, et al. Efficient light harvesting by using green Zn-porphyrin-sensitized nanocrystalline TiO_2 films. Journal of Physical Chemistry B 2005;109:15397–409.
[28] Nogueira AF, Furtado LFO, Formiga ALB, Nakamura M, Araki K, Toma HE. Sensitization of TiO_2 by supramolecules containing zinc porphyrins and ruthenium-polypyridyl complexes. Inorganic Chemistry 2004;43:396–8.
[29] Cherian S, Wamser CC. Adsorption and photoactivity of tetra(4-carboxyphenyl) porphyrin (TCPP) on nanoparticulate TiO_2. Journal of Physical Chemistry B 2000;104:3624–9.
[30] Rochford J, Chu D, Hagfeldt A, Galoppini E. Tetrachelate porphyrin chromophores for metal oxide semiconductor sensitization: effect of the spacer length and anchoring group position. Journal of the American Chemical Society 2007;129:4655–65.
[31] Molinari A, Amadelli R, Antolini L, Maldotti A, Battioni P, Mansuy D. Photoredox and photocatalytic processes on Fe(III)–porphyrin surface modified nanocrystalline TiO_2. Journal of Molecular Catalysis A 2000;158:521–31.
[32] Eu S, Hayashi S, Umeyama T, Oguro A, Kawasaki M, Kadota N, et al. Effects of 5-membered heteroaromatic spacers on structures of porphyrin films and photovoltaic properties of porphyrin-sensitized TiO_2 cells. Journal of Physical Chemistry C 2007;111:352837.
[33] Balaban TS. Tailoring porphyrins and chlorine for self-assembly in biomimetic artificial antenna systems. Accounts of Chemical Research 2005;38:612–23.
[34] Ramakrishna G, Verma S, Amilan JD, Krishna KD, Das A, Palit DK, et al. Interfacial electron transfer between the photoexcited porphyrin molecule and TiO_2 nanoparticles: effect of catecholate binding. Journal of Physical Chemistry B 2006;110:9012–21.
[35] Deng HH, Lu ZH, Shen YC, Mao HF, Xu HJ. Improvement in photoelectric conversion of a phthalocyanine-sensitized TiO_2 electrode by doping with porphyrin. Chemical Physics 1998;231:95–103.
[36] Nagata T, Kikuzawa Y. An approach towards artificial quinone pools by use of photoand redox-active dendritic molecules. Biochimica et Biophysica Acta 2007;1767:648–52.
[37] Banfi S, Cassani E, Caruso E, Cazzaro M. Oxidative cleavage of plasmid bluescript by water-soluble Mn–porphyrins and artificial oxidants or molecular oxygen. Bioorganic and Medicinal Chemistry 2003;11:3595–605.
[38] Gervaldo M, Fungo F, Durantini EN, Silber JJ, Sereno L, Otero L. Carboxyphenyl metalloporphyrins as photosensitizers of semiconductor film electrodes. a study of the effect of different central metals. Journal of Physical Chemistry B 2005;109:209530–62.
[39] Mele G, Elisa GL, Leonardo P, Dyrda G, Sıota R. Photocatalytic degradation of 4-nitrophenol in aqueous suspension by using polycrystalline TiO_2 impregnated with lanthanide double-decker phthalocyanine complexes. Journal of Physical Chemistry C 2007;111:6581–8.
[40] Marvel CS, Tanenbaum AL. The preparation of 1,4-dihalogen derivatives of butane. Journal of the American Chemical Society 1922;44:2645–50.
[41] Wang C, Li J, Yang GM, Mele G, Zhang FX, Palmisano L, et al. Efficient degradation of 4-nitrophenol by using functionalized porphyrin–TiO_2 photocatalysts under visible irradiation. Applied Catalysis B Environmental 2007;76:218–26.
[42] Becke AD. Journal of Chemical Physics 1993;98:1372–7.
[43] Lee C, Yang W, Parr RG. Physical Review B 1988;37:785–9.
[44] Frisch MJ, Trucks GW, Schlegel HB, Scuseria GE, Robb MA, Cheeseman JR, et al. Gaussian 03, Revision B.04. Pittsburgh PA: Gaussian, Inc.; 2003.
[45] Wadt WR, Hay PJ. Journal of Chemical Physics 1985;82:284–98.
[46] Lindesy JS, Schreiman IC, Hsu HC, Kearney PC, Marguerettaz AM. Rothemund and Adler–Longo reactions revisited: synthesis of tetraphenylporphyrins under equilibrium conditions. Journal of Organic Chemistry 1987;52:827–36.
[47] Mele G, Del Sole R, Vasapollo G, García-López E, Palmisano L, Li J, et al. TiO_2-based photocatalysts impregnated with metallo-porphyrins employed for degradation of 4-nitrophenol in aqueous solutions: role of metal and macrocycle. Research on Chemical Intermediates 2007;33:433–48.